

## 2. A unique volcanic field in Tharsis, Mars: Pyroclastic cones as evidence for explosive eruptions

*Petr Brož<sup>1,2</sup> and Ernst Hauber<sup>3</sup>*

*<sup>1</sup>Institute of Geophysics ASCR, v.v.i., Prague, Czech Republic*

*<sup>2</sup>Institute of Petrology and Structural Geology, Faculty of Science, Charles University, Prague, Czech Republic*

*<sup>3</sup>Institute of Planetary Research, DLR, Berlin, Germany*

**Status:** Published in Icarus 218(1), doi: 10.1016/j.icarus.2011.11.030.

### 2.0. Abstract

Based on theoretical grounds, explosive basaltic volcanism should be common on Mars, yet the available morphological evidence is sparse. We test this hypothesis by investigating a unique unnamed volcanic field north of the shield volcanoes Biblis Patera and Ulysses Patera on Mars, where we observe several small conical edifices and associated lava flows. Twenty-nine volcanic cones are identified and the morphometry of many of these edifices is determined using established morphometric parameters such as basal width, crater width, height, slope, and their respective ratios. Their morphology, morphometry, and a comparison to terrestrial analogs suggest that they are martian equivalents of terrestrial pyroclastic cones, the most common volcanoes on Earth. The cones are tentatively interpreted as monogenetic volcanoes. According to absolute model age determinations, they formed in the Amazonian period. Our results indicate that these pyroclastic cones were formed by explosive activity. The cone field is superposed on an old, elevated window of fractured crust which survived flooding by younger lava flows. It seems possible that a more explosive eruption style was common in the past, and that wide-spread effusive plain-style volcanism in the Late Amazonian has buried much of its morphological evidence in Tharsis.

## 2.1. Introduction and background

Most volcanoes on Mars that have been studied so far seem to be basaltic shield volcanoes (e.g., Mouginis-Mark et al., 1992; Zimbelman, 2000), which can be very large with diameters of hundreds of kilometers (Plescia, 2004) or much smaller with diameters of several kilometers only (Hauber et al., 2009a). The eruptive style of the large shields, at least in the later part of martian history, was early interpreted to be predominantly effusive (Greeley, 1973; Carr et al., 1977; Greeley and Spudis, 1981), although theoretical considerations predict that basaltic explosive volcanism should be common on Mars (Wilson and Head, 1994). Unequivocal evidence for explosive volcanism on Mars is rare and mainly restricted to ancient terrains. Some of the old highland paterae (e.g., Hadriaca, Tyrrhena, and Apollinaris Paterae; >3.5 Ga) display easily erodible and very shallow flanks that were interpreted to be composed of airfall and pyroclastic flow deposits (Greeley and Crown, 1990; Crown and Greeley, 1993; Gregg and Williams, 1996; Gregg and Farley, 2006; Williams et al., 2007, 2008). Widespread layered deposits in the equatorial regions of Mars, e.g., the Medusae Fossae Formation, were interpreted to be pyroclastic deposits (Chapman, 2002; Hynek et al., 2003; Mandt et al., 2008; Kerber et al., 2010), but their nature and timing are not well understood.

Pyroclastic cones, defined in this study as scoria, cinder, or tephra cones (Vespermann and Schmincke, 2000), are the most common type of terrestrial volcanoes (Wood, 1979a,b) and were suggested by several authors already decades ago to exist on Mars (e.g., Wood, 1979b; Dehn and Sheridan, 1990). However, only few Viking Orbiter-based studies reported their possible existence near the caldera of Pavonis Mons, on the flanks of Alba Patera, in the caldera of Ulysses Patera, and in the Cydonia and Acidalia regions (Carr et al., 1977; Wood, 1979a,b; Frey and Jarosewich, 1982; Edgett, 1990; Hodges and Moore, 1994; Plescia, 1994). It was recognized that this might have been an observational effect caused

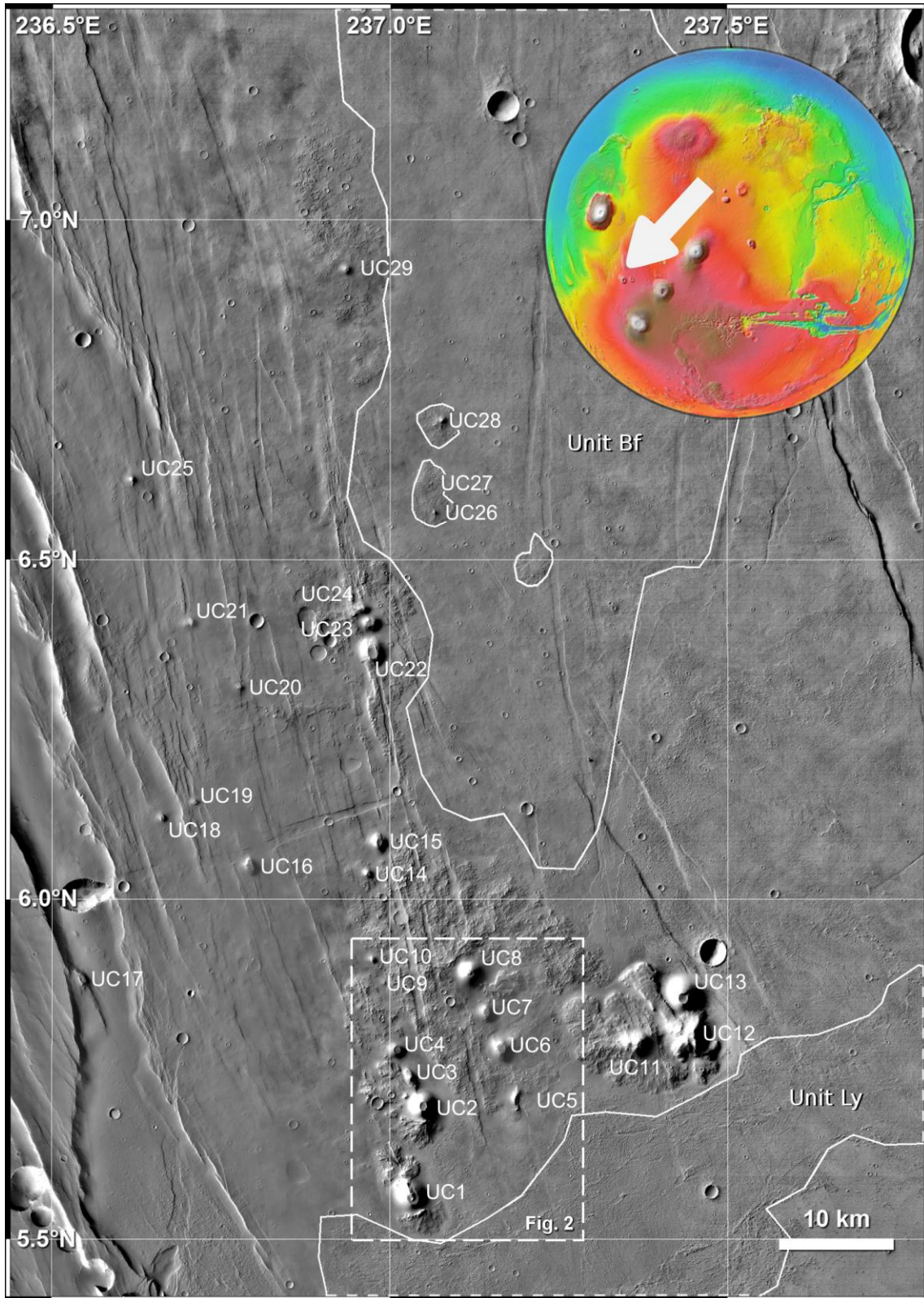


Figure 2.1. Mosaic of CTX and HRSC images showing all investigated cones. Cone IDs are the same as used in Tab. 2.2 (CTX images B17\_016134\_1842, P19\_008262\_1862, P22\_009554\_1858 and image HRSC h8396\_0009). Dashed line shows location of Fig. 2.2. Cf and Ly represent areas for crater counting. See text for more details.

by the relatively low image resolution of the Viking Orbiter cameras (typically 60-100 m/pixel), and Zimbelman (2000) presumed that many small domes on Mars might have a volcanic origin. It was indeed only the advent of higher-resolution data that led to the interpretation of previously unknown edifices as rootless cones (Fagents and Thordarson, 2007; Keszthelyi et al., 2010) or scoria cones (Bleacher et al., 2007, Keszthelyi et al., 2008; Lanz et al., 2010), but without in-depth analyses of their origin. A volcanic cone in the caldera of Nili Patera, part of the Syrtis Major volcanic complex, is associated with a lava flow and silica deposits that might be the result of hydrothermal activity (Skok et al., 2010). Ground-based observations by the Mars Exploration Rover, Spirit, revealed further morphologic evidence ('bomb sags') for explosive volcanic activity (Squyres et al., 2008).

Pyroclastic cones have not yet been described and measured in detail on the martian surface. Previous studies were mostly based on low-resolution Viking data that did not allow the description of individual cones, or high-resolution studies that discussed only isolated features. Only Lanz et al. (2010) were able to provide quantitative analyses of multiple cones in a high-resolution study of a possible volcanic rift zone in SW Utopia Planitia. They investigated an area exhibiting scoria cones and associated lava flows, and measured the crater and basal diameters of putative scoria cones, which they compared with other cones surrounding their study area.

The identification of pyroclastic cones can constrain the nature of associated eruption processes and, indirectly, improve our understanding of the nature of parent magmas (e.g., volatile content; Roggensack et al., 1997). Moreover, the morphometry and spatial distribution of pyroclastic cones can reveal tectonic stress orientations (Nakamura, 1977; Tibaldi, 1995) and the geometry of underlying feeder dikes (Corazzato and Tibaldi, 2006). Hence, pyroclastic cones on Mars are therefore potentially interesting study objects, and the increasing amount of high-resolution data enables their detailed analysis. We test

Table 2.1. Table of image scenes used for this study (pixel resolution, imaging time, and illumination geometry). †HiRISE resolutions are given for map-projected images.

Image ID	Ground pixel resolution	Acquisition time	Solar elevation above horizon	Solar azimuth (for map projected image)
h1012_0000	11.8 m pixel <sup>-1</sup>	02 Nov 2004	36°	295.0
h1023_0000	11.5 m pixel <sup>-1</sup>	05 Nov 2004	37°	295.1
P19_008262_1862	5.51 m pixel <sup>-1</sup>	01 May 2008	41°	277.03°
P21_009198_1858	5.42 m pixel <sup>-1</sup>	13 Jul 2008	38°	277.12°
P21_009409_1858	5.53 m pixel <sup>-1</sup>	29 Jul 2008	37°	277.05°
P22_009554_1858	5.53 m pixel <sup>-1</sup>	09 Aug 2008	38°	277.21°
B17_016134_1842	5.35 m pixel <sup>-1</sup>	04 Jan 2010	48°	277.09°
B12_014156_1857	5.46 m pixel <sup>-1</sup>	03 Aug 2009	49°	277.12°
PSP_008262_1855†	50 cm pixel <sup>-1</sup>	01 May 2008	41°	277°
PSP_009198_1860†	50 cm pixel <sup>-1</sup>	13 Jul 2008	38°	277.12°
PSP_009409_1860†	50 cm pixel <sup>-1</sup>	29 Jul 2008	37°	277.05°
PSP_009554_1860†	25 cm pixel <sup>-1</sup>	09 Aug 2008	38°	277.21°

the hypothesis that explosive basaltic volcanism should be common on Mars and report on our investigation of a unique unnamed cluster of possible volcanic cones situated north of Biblis Patera in the Tharsis region (Fig. 2.1). To our knowledge, this is the first ever study of this unique volcanic field.

## 2.2. Data and methods

This study uses imaging data from several cameras, i.e. ConTeXt Camera (CTX; Malin et al., 2007), High Resolution Stereo Camera (HRSC; Jaumann et al., 2007), and High Resolution Imaging Science Experiment (HiRISE; McEwen et al., 2007) (Tab. 2.1). CTX images have sufficient resolution (5-6 meters/pixel) to identify possible scoria cones, associated lava flows and their relationships to the geological context. On the other hand, HiRISE data were used to investigate small details of cones in very high spatial resolution. Topographic information (e.g., heights and slope angles) were determined from single shots of the Mars Orbiter Laser Altimeter (MOLA; Zuber et al., 1992; Smith et al., 2001) in a GIS environment, and from stereo images (HRSC, CTX) and derived gridded digital elevation

models (DEM). An anaglyph image made from two HiRISE observations provided qualitative topographic information.

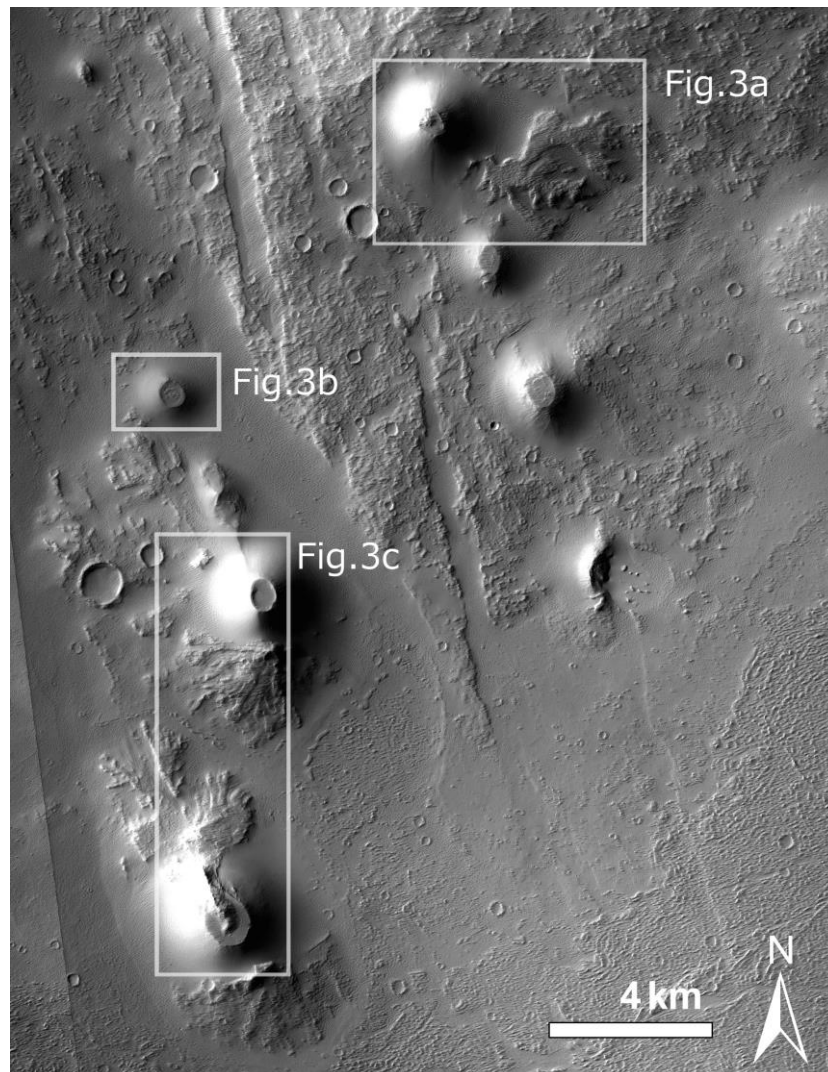


Figure 2.2. Selected cones and associated flows emanating from the cones in the study area. The distribution of cones is controlled by NW-trending extensional fault systems (CTX image P19\_008262\_1862, image center at 5.75°N/237.1°E; see Fig. 2.1 for location).

### 2.3. Regional setting

The study area is situated within the Tharsis volcanic province, the largest known volcano-tectonic province on Mars (Fig. 2.1). It is located at the southeastern margin of the several hundred kilometer-long fault system, Ulysses Fossae, and north of two

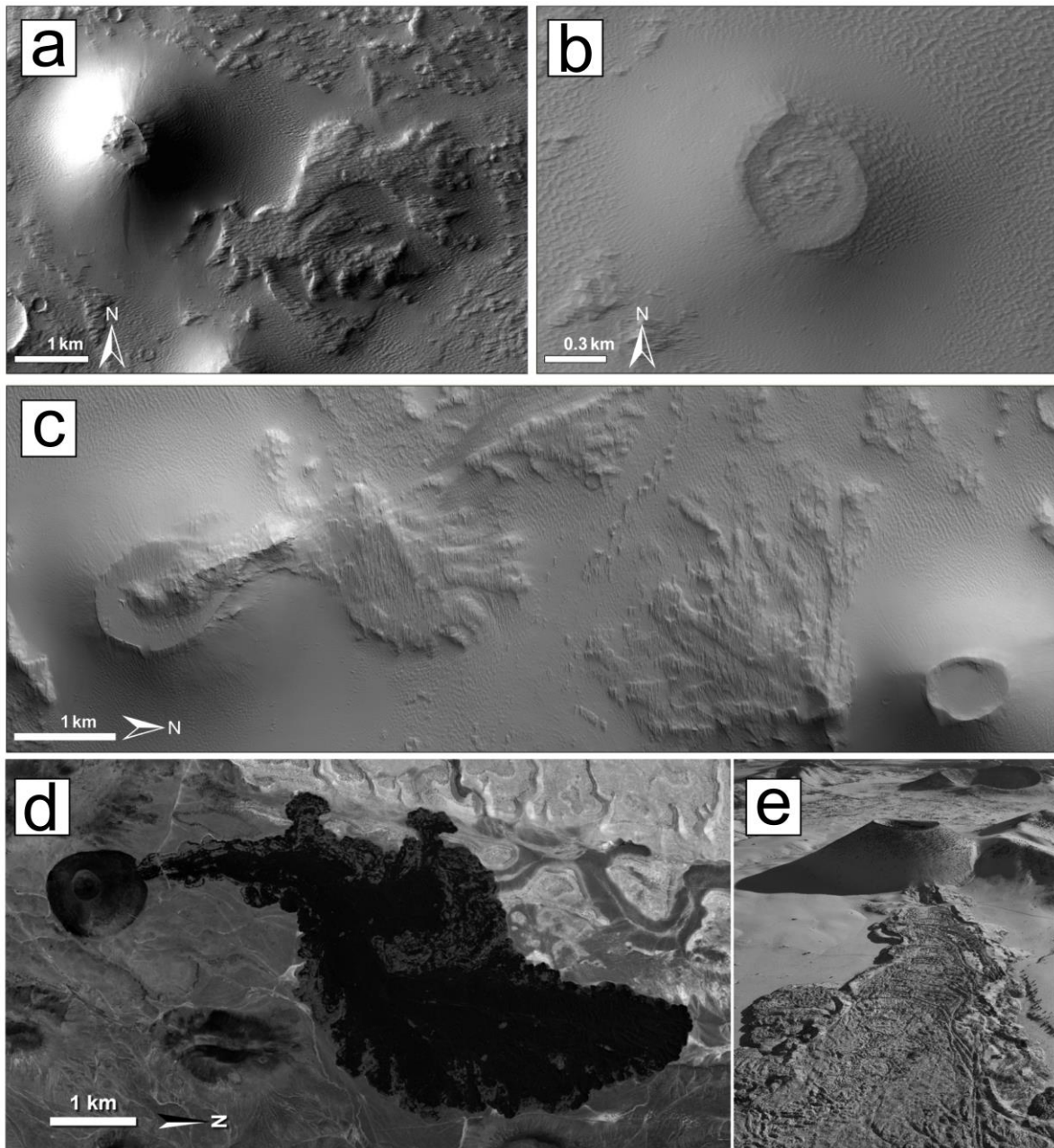


Figure 2.3. (a) Detail of lobate flow-like deposit starting at the base of a cone (detail of CTX P22\_009554\_1858, centered at  $5.87^{\circ}\text{N}/237.15^{\circ}\text{E}$ ). (b) Summit crater of cone with well-developed rim and flat summital plateau (detail of HiRISE PSP\_008262\_1855, centered at  $5.78^{\circ}\text{N}/237.01^{\circ}\text{E}$ ). (c) Flow-like deposits with branching morphology. One flow originates from a fissure-like source cutting a cone (right), another flow originates at the lower flank of a cone (lower left). Note that the transition between the flows and the surrounding terrain is partly obscured by a thick dust layer (detail of HiRISE PSP\_008262\_1855, centered at  $5.65^{\circ}\text{N}/237.02^{\circ}\text{E}$ ). (d) Terrestrial cinder cone with associated lava flow in plan view (SP Mountain, Arizona, USA; image: NASA). (e) Oblique aerial view of the same cinder cone with detail of lava flow in the foreground (image: Michael Collier).

large volcanoes, Biblis and Ulysses Paterae. The Ulysses Fossae itself represent a window of older crust, probably of early Hesperian age (Anderson et al., 2001), which survived later resurfacing of large younger lava flows (Scott and Tanaka, 1986). The investigated area seems to be part of this older crust, which is partly embayed by younger lava material.

The study area is structurally characterized by extensive N- to NNW-trending normal faults, which often form grabens that dissect especially the northern and western part of it (Scott and Dohm, 1990). The southern and eastern parts are covered by younger lava flows that had their origin towards the southeast. Most of the topographic edifices are observed close to the transition between the younger lava flows and the older heavily fractured crust. The spatial arrangement of the edifices is obviously controlled by the fault trend, and single edifices appear aligned along faults, building small clusters (Fig. 2.1 and 2.2). Several cones grew on older deposits with a rough texture that partly buries the underlying faults. Parts of these rough deposits are disrupted by faults, however, suggesting a later reactivation of faulting (Fig. 2.1 and 2.2). Close inspection of HiRISE images suggests that the entire area is thickly mantled by dust.

## **2.4. Morphology**

A total of 29 possible volcanic edifices were identified. These cones are spread over an area of about  $50 \times 80$  kilometers, with the main clustering of edifices in the south and several widely spread cones in the north (see Fig. 2.1 for the detailed spatial distribution of cones). All the measured dimensions of the cones increase from North to South. The more southern edifices are also better preserved, with well-developed morphologies of truncated cones and uniform flank slopes. In contrast, the northern cones are smaller and appear degraded without preserved visible craters on their top. In plan view, the cone morphology is characterized by circular to elongated outlines (Fig. 2.3a and 2.3b), relatively steep-appearing

Table 2.2. All measured values of investigated volcanic cones. Positions are drawn in Fig. 2.1 for each cone.

ID	$W_{co}$ average [m]	$W_{cr}$ average [m]	$H_{co}$ [m]	$W_{cr}/W_{co}$	$H_{co}/W_{co}$	Slope [°]	Volume [km <sup>3</sup> ]
A1	3909	1185	539	0.30	0.14	21.60	3.01
A2	3219	721	651	0.22	0.20	27.53	2.25
A3	-	-	-	-	-	-	-
A4	1785	606	130	0.34	0.07	12.43	0.16
A5	-	-	-	-	-	-	-
A6	2891	779	314	0.27	0.11	16.56	0.92
A7	2258	638	-	0.28	-	-	-
A8	3311	637	422	0.19	0.13	17.51	1.49
A9	-	-	-	-	-	-	-
A10	-	-	88	-	-	-	-
A11	2968	732	519	0.25	0.17	24.90	1.56
A12	-	-	-	-	-	-	-
A13	3694	883	-	0.24	-	-	-
A14	1092	401	120	0.37	0.11	19.15	0.06
A15	1715	665	180	0.39	0.10	18.92	0.21
A16	1964	795	164	0.40	0.08	15.68	0.26
A17	-	598	-	-	-	-	-
A18	-	365	82	-	-	-	-
A19	-	304	83	-	-	-	-
A20	-	-	112	-	-	-	-
A21	1507	390	-	0.26	-	-	-
A22	2904	1147	292	0.39	0.10	18.38	1.00
A23	2150	609	250	0.28	0.12	17.97	0.41
A24	1325	454	129	0.34	0.10	16.49	0.09
A25	-	-	125	-	-	-	-
A26	-	-	64	-	-	-	-
A27	-	-	-	-	-	-	-
A28	980	183	150	0.19	0.15	20.62	0.05
A29	1452	281	180	0.19	0.12	17.08	0.38

flanks, and summit craters or plateaus (Fig. 2.3b). Some cones are associated with lobate and sometimes branching deposits, which emanate from the summit craters or from some points at or very near the flanks (Fig. 2.3a and 2.3c). The outline of these features in plan view

resembles that of lobate flows. The flow-like features appear to be rather short and thick, as compared to most lava flows in Tharsis and Elysium. A thick dust cover, which is typical for Tharsis and hinders the full exploitation of the very high spatial resolution of HiRISE (Keszthelyi et al., 2008), prevents the identification of meter-scale textural details of the cones and the associated lobate flows. Both cones and associated flows are superposed on terrain with a rough texture that forms local topographic bulges.

The cones and flows are much better preserved than recently detected cones and flows in Utopia (Lanz et al., 2010). The association of cones with lobate flows distinguishes these cones from other cone fields on Mars, which were mostly interpreted as clusters of rootless cones (Frey and Jarosewich, 1982; Fagents and Thordarson, 2007; Lanagan et al., 2001). Interestingly, however, none of the craters on top of the cones is breached by a lava flow, which is a common situation for terrestrial pyroclastic cones (Wood, 1980a; Head and Wilson, 1989). Pyroclastic cones observed by Bleacher et al. (2007) and Keszthelyi et al. (2008) are breached, but no associated flows could be identified. Our observations reveal that at least three cones are associated with flows starting at the base of cones or on their flanks.

## **2.5. Morphometry**

Our investigation is based on measurements of basic morphologic properties of identified cones, which were previously used for terrestrial pyroclastic cones and other types of volcanic edifices (e.g., Porter, 1972; Settle, 1979; Wood, 1979a, Hasenaka and Carmichael, 1985b; for a review of previous studies on volcano morphometry see Grosse et al., 2012). Cone diameter ( $W_{CO}$ ) and crater diameter ( $W_{CR}$ ) were determined by averaging four measurements in different directions. Cone height ( $H_{CO}$ ) was obtained from MOLA single tracks or from HRSC DEM. These basic parameters were used to calculate two basic ratios,  $W_{CR}/W_{CO}$  and  $H_{CO}/W_{CO}$ , and the slope angle (Porter, 1972; and references therein).

The volume was calculated via the equation for a truncated cone, also used by Hasenaka and Carmichael (1985a):

$$V = (\pi H_{CO} / 3) (R_{CR}^2 + R_{CR} R_{CO} + R_{CO}^2) \quad (2.1)$$

where the radii,  $R_{CR}$  and  $R_{CO}$ , are  $0.5 W_{CR}$  and  $0.5 W_{CO}$ , respectively. It was possible to measure the morphometric properties for almost half of the 29 cones (Tab. 2.2). Burial of the lower parts of cones by later lava flows would imply that we only measured the apparent basal diameter after embayment and a correspondingly smaller height, but based

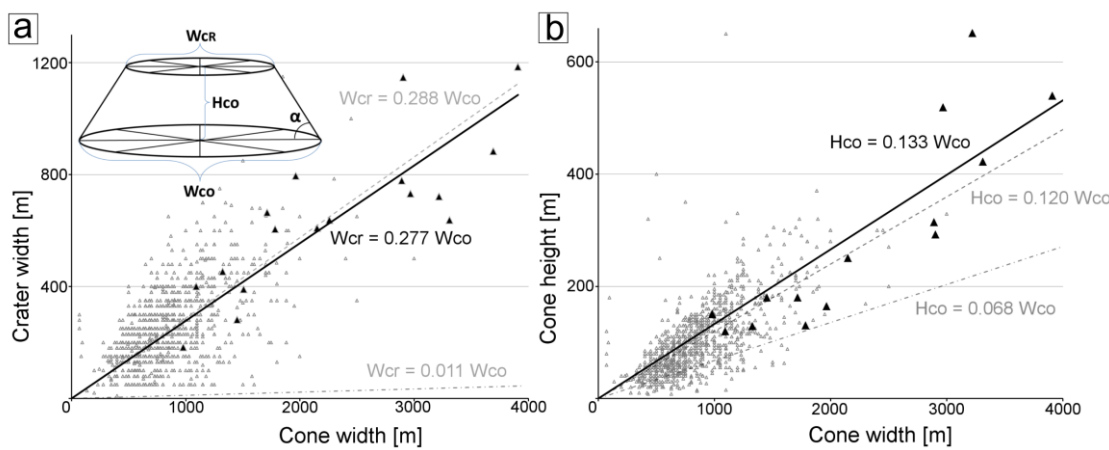


Figure 2.4. Morphometry of investigated cinder cones in comparison with terrestrial cinder cones and stratovolcanoes with summit craters. Full triangles correspond to investigated Martian cones; empty triangles to terrestrial cinder cones (~1060 edifices from Hasenaka and Carmichael, 1985a; Inbar and Risso, 2001; Pike, 1978). The inset in A illustrates the morphometric parameters used in this study.  $W_{CO}$  is basal width of cone,  $H_{CO}$  cone height,  $W_{CR}$  represents the basal crater diameter, and  $\alpha$  is the slope angle. (a) Plot of summit crater width ( $W_{CR}$ ) versus basal cones width ( $W_{CO}$ ) of cones. The solid line represents the best fit (linear regression) for Martian cones with a value  $W_{CR}/W_{CO} = 0.277$ . Terrestrial cinder cones are represented by dashed line ( $W_{CR}/W_{CO} = 0.288$ ), and for comparison the dotted-and-dashed line represents terrestrial stratovolcanoes with summit craters ( $W_{CR}/W_{CO} = 0.011$ ). (b) Plot of cone height ( $H_{CO}$ ) versus basal width of cone. Lines represent the same edifices as in plot a. Both plots demonstrate the morphometrical similarity between Martian cones and terrestrial cinder cones.

on the visual appearance of the cones we consider this possible effect to be insignificant. The morphometry of terrestrial monogenetic volcanic landforms was previously determined (e.g., Wood, 1979a or Tab. 2.3). In particular, Wood (1980a) reports the morphometry of 910 scoria cones from different volcanic fields. Scoria cones on Earth have a mean basal diameter of 900 m, but can range widely in dimension (Wood; 1980a). The ratio between crater diameter and basal diameter has an average value of 0.4 (Wood, 1980a; Porter, 1972),

Table 2.3. Comparison of morphometric data (mean values) of pyroclastic cones on Earth and Mars.  $N$ -number of cones,  $W_{CO}$ -width of cone,  $W_{CR}$ -width of crater,  $H_{CO}$ -height of cone.

Volcanic field or region	N	$W_{CO}$ [m]	$W_{CR}$ [m]	$H_{CO}$ [m]	$W_{CR}/W_{CO}$	$H_{CO}/W_{CO}$	Volume [km <sup>3</sup> ]	Source <sup>(1)</sup>
Mauna Kea (Hawaii)	-	-	115 <sup>(2)</sup>	-	0.4	0.18	-	[1]
Michoacán- Guanajuato (Mexico)	901	830	240	100	-	-	0.038	[2]
Michoacán- Guanajuato (Mexico)	11	950	308	170	0.32	0.17	0.07	[3]
Xalapa (Mexico)	57	698	214	90	0.3	0.14	0.13	[4]
Payun Matru (Argentina)	120	1,100	306	127	0.32 <sup>(3)</sup>	0.13	-	[5]
Kamtchatka (Russia)	9	795	n.a.	149	-	0.18	0.07	[6]
Lamongan (Indonesia)	36	760	77 <sup>(4)</sup>	94	0.19 <sup>(4)</sup>	0.13 <sup>(5)</sup>	0.039	[7]
Ulysses Fossae (Mars)	29	2,300	620	230	0.28	0.13	0.85	this study

<sup>(1)</sup> [1] Porter (1972). [2] Hasenaka and Carmichael (1985a). [3] Hasenaka and Carmichael (1985b).

[4] Rodriguez et al., 2010. [5] Inbar and Risso (2001). [6] Inbar et al. (2011). [7] Carn (2000).

<sup>(2)</sup> measured for 218 cones (see Fig. 3 of Porter, 1972).

<sup>(3)</sup> only determined for 76 cones for which a crater diameter is given by Risso and Inbar (2001).

<sup>(4)</sup> determined for 14 cones.

<sup>(5)</sup> determined for 27 cones

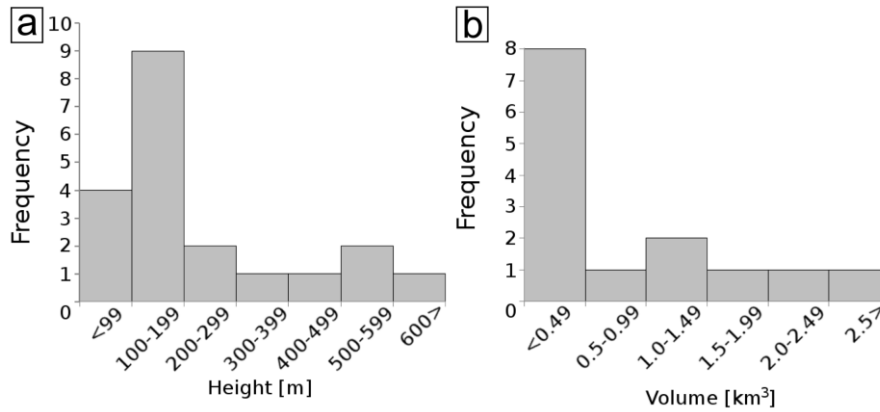


Figure 2.5. a) Histogram of cones heights. (b) Histogram of cone volumes.

but other studies including scoria cones in different stages of erosion show a lower value for this ratio (see Fig. 2.4a, black dashed line). The height of fresh scoria cones on Earth is equivalent to  $0.18 W_{CO}$  (Porter, 1972; Wood, 1980a), but the height distribution has a wide range towards lower values.

Our measurements suggest that the cones in the study area have a mean basal diameter of 2300 m, with a range from ~1000 to ~3900 m. This is about ~2.6 times larger than the basal diameter of terrestrial pyroclastic cones and also larger than the scoria cones reported by Lanz et al. (2010) in Utopia Planitia (~280 to 1000 m). The crater diameter for the cones studied here ranges from ~185 to ~1185 m, with an average of 650 m, which is about ~2.5 times larger than terrestrial pyroclastic cones (average ~257 m). It is also larger than that of the scoria cones reported by Lanz et al. (2010) (110 to 450 m). The  $W_{CR}/W_{CO}$  ratio of the investigated cones has a mean value of 0.277. The edifices are also higher (from 64 to 651 m; Fig. 2.5a) than terrestrial pyroclastic cones (average height: 105 m, based on measurements of 1063 edifices, data from Hasenaka and Carmichael, 1985b; Inbar and Risso, 2001; and Pike, 1978; for additional morphometric measurements of terrestrial pyroclastic cones see Rodriguez et al., 2010). The  $H_{CO}/W_{CO}$  ratio is 0.133 (Fig. 2.4b), which is less than that of pristine terrestrial pyroclastic cones with a ratio of 0.18. The slope

distribution of cone flanks is between  $12^\circ$  and  $27.5^\circ$  (the steepest sections reach  $>30^\circ$ ), with higher values for well-preserved cones with associated flow-like features and lower values corresponding to more degraded edifices. These values are in agreement with slope angles for terrestrial pyroclastic cones in different stages of erosion, with older and more eroded cones exhibiting progressively lower slope angles (Hooper and Sheridan, 1998). The volume is ranging from 0.05 to  $3.01 \text{ km}^3$  (Fig. 2.5b), while the average terrestrial value is  $0.046 \text{ km}^3$  (determined from 986 edifices, data from Pike, 1978; Hasenaka and Carmichael, 1985b). The volume of the cones in the study area is mostly one to two orders of magnitude higher than that of pyroclastic cones on Earth.

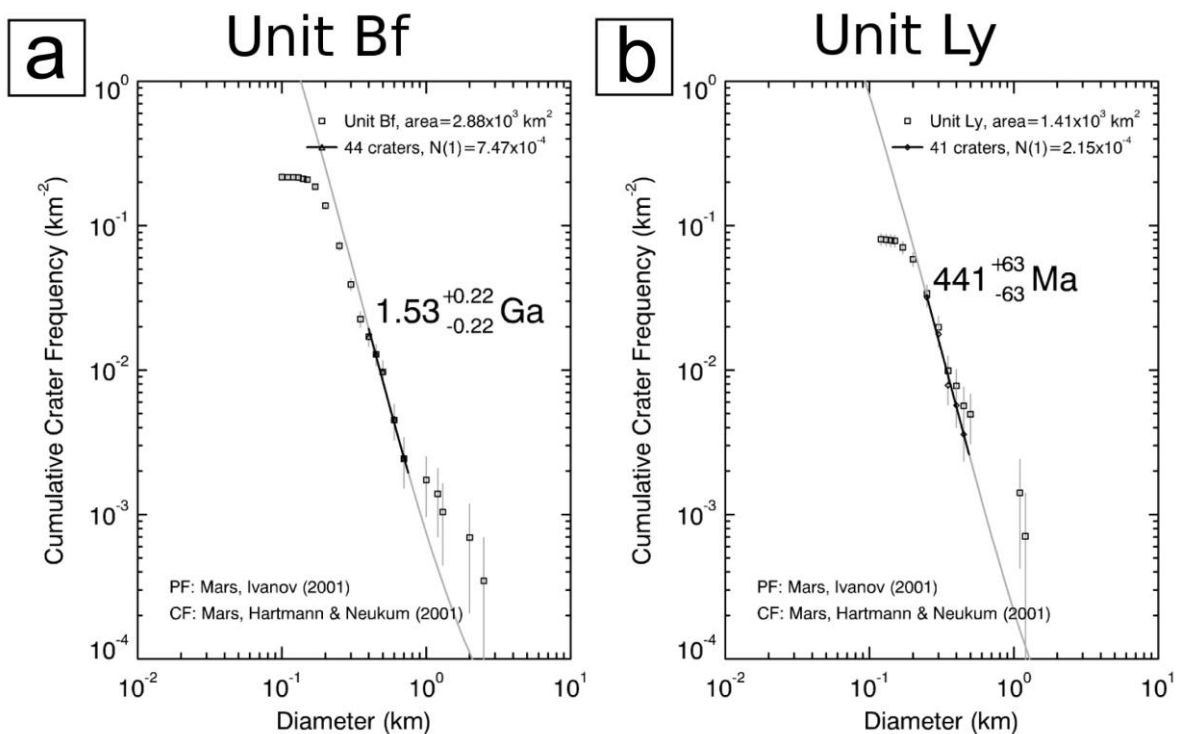


Figure 2.6: Absolute model ages for two surface units which are interpreted to be older and younger than the volcanic cones, thereby bracketing the age of volcanic activity. (a) Crater size-frequency distribution of the fractured basement (Unit Bf) on which the volcanic field was emplaced. The cumulative crater curve indicates an absolute model age of  $\sim 1.5 \text{ Ga}$ . (b) Same for the lava flows (unit Ly) that embay the volcanic field in the southeast. The absolute model age is about  $440 \text{ Ma}$ . See Fig. 2.1 for location of units Bf and Ly.

## 2.6. Age

The absolute model age determination of planetary surfaces uses the crater size-frequency distribution as measured on images (Crater Analysis Techniques Working Group, 1979). The small size of, and the thick dust cover on the cones prevent the counting of small craters on the cones themselves. Moreover, their shape with slope angles of up to  $30^\circ$  renders them useless for crater counting, since gravitational movements on the slopes would cause distortions of the original geometry of impact craters. Instead, we dated two areas (*cf.* Fig. 2.1) which we consider to be older and younger than the cones, thus bracketing their formation age. One of these areas is the faulted basement, which by definition is older than the faulting and, therefore, older than the cones. The other area represents the lava flows in the southeast, which embay the topographic high and are assumed to be younger than the cones. Representative surface areas for age determinations were mapped and craters counted on CTX images utilizing the software tool ‘cratertools’ (Kneissl et al., 2011). Absolute crater model ages were derived with the software tool ‘craterstats’ (Michael and Neukum, 2010) by analysis of crater-size frequency distributions applying the production function coefficients of Ivanov (2001) and the impact-cratering chronology model coefficients of Hartmann and Neukum (2001). We determined absolute model ages of  $\sim 1.5$  Ga and  $\sim 0.44$  Ga for the older and the younger area, respectively, thus the formation of the cones probably occurred within this time interval (Fig. 2.6). This method of absolute age range determination can not reveal any age differences between individual cones (see below), since no degradational sequence can be inferred from the observed unit relationships.

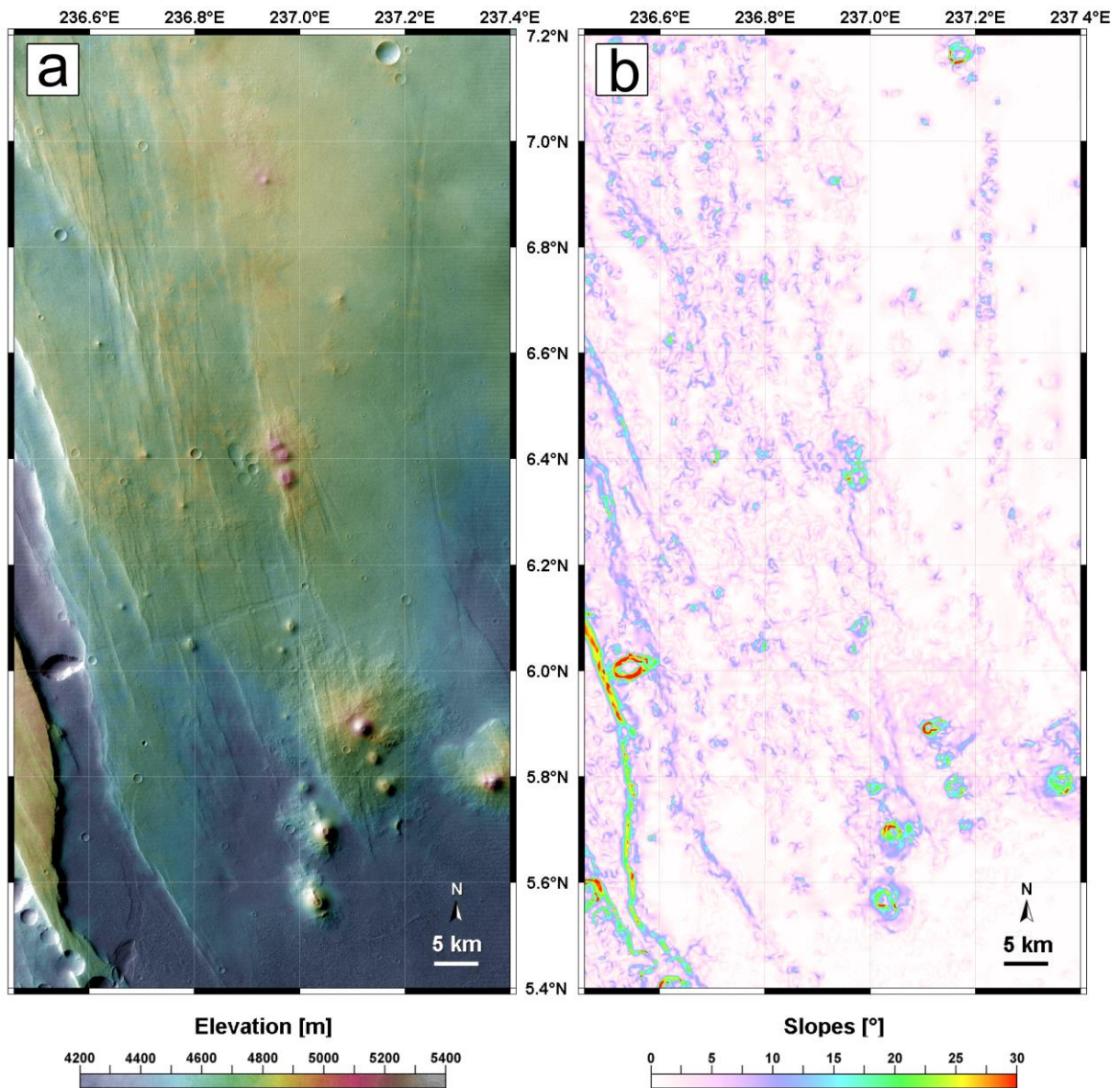


Figure 2.7: (a) Topographic map of western part of the study area. (b) Slope map. Note that the substrate on which the cones are superposed has very low slope angles, and therefore does not affect the morphometry of the cones (cf. Tibaldi, 1995, who noted that substrate slopes  $>9^\circ$  can affect cone morphometry). Both maps were derived from HRSC image sequence h1023\_0000.

## 2.7. Discussion

Some morphological and morphometrical characteristics of the cones in the study area suggest an origin as pyroclastic cones. Their appearance as truncated cones with smooth

flanks of more or less uniform slope angles, summit craters or plateaus, and associated flows is analogous to terrestrial scoria or cinder cones associated with lava flows (Fig. 2.3). The most striking morphometric similarity between the martian cones and terrestrial scoria cones is the  $W_{CR}/W_{CO}$  ratio (Fig. 2.5a). It is clearly distinguished from that of terrestrial stratovolcanoes, which has typically values of  $\sim 0.027$  (McKnight and Williams, 1997). The influence of preexisting topography on cone morphology is negligible. Tibaldi (1995) reports that substrate slopes  $<9^\circ$  do not affect cone shapes. Topographic and slope maps of the study area (Fig. 2.7) show that the substrate has slopes  $<9^\circ$  throughout the study area. Other morphometric parameters of the studied cones, however, are different from terrestrial pyroclastic cones, e.g., the basal diameter and the height. Theoretical considerations predict considerable differences between pyroclastic (scoria) cones on Earth and Mars (for a given magma volume and volatile content), due to the specific surface environment on both planets, in particular gravity and atmospheric pressure (Wilson and Head, 1994). Pyroclastic cones on Mars should have larger basal diameters and lower heights (Wilson and Head, 1994; Fagents and Wilson, 1996; Parfitt and Wilson, 2008), and the  $W_{CR}/W_{CO}$  ratio should be larger (Wilson and Head, 1994). However, Wood (1979b) assumed that this ratio is independent of gravity and atmospheric pressure, because the wider dispersal of ejecta material would affect crater width and basal diameter in the same way. Therefore,  $W_{CR}/W_{CO}$  should be the same for pyroclastic cones on Earth, Mars or others bodies. Dehn and Sheridan (1990) theoretically modeled pyroclastic cones on different terrestrial bodies, and they predicted that basal diameters of pyroclastic cones on Mars should be 2 to 3 times larger than those of terrestrial pyroclastic cones. The same authors also suggest that the cones should be  $>100$  m high and display well-developed deep central craters. Our measurements show cone basal diameters  $\sim 2.6$  times larger than for typical terrestrial scoria cones, fitting

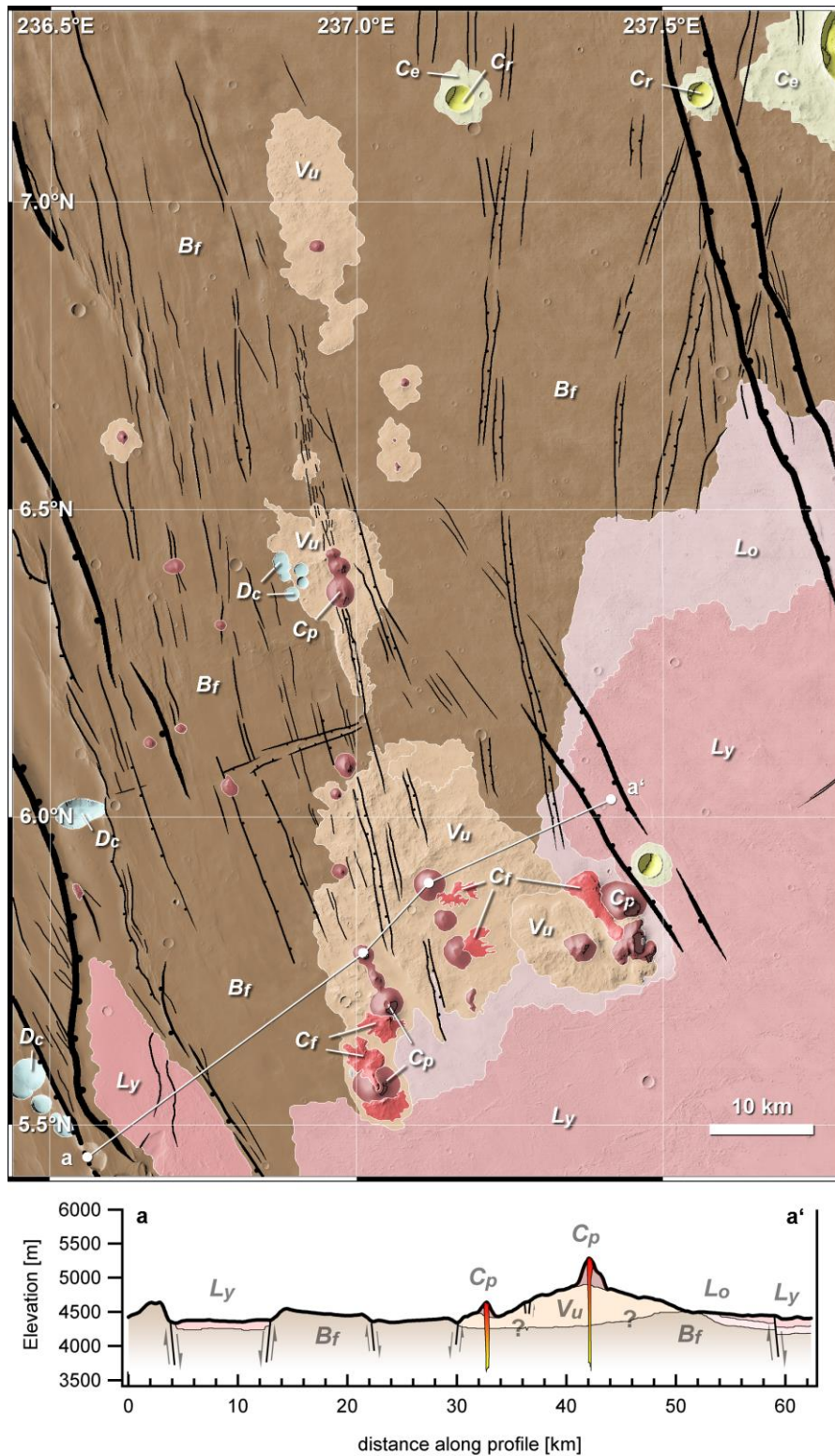


Figure 2.8: Schematic geological and structural map. Units: *Cp*-pyroclastic cone; *Cf*-Lava flows associated with pyroclastic cones; *Vu*-volcanic deposits (unclassified); *Dc*-collapse depressions, *Lo*-older lava flows; *Ly*-younger lava flows; *Bf*-fractured basement; *Cr*-large crater; *Ce*-crater ejecta. Black lines with hatches on one side: grabens, dipping toward hatched side; other black lines: fractures (mostly normal faults).

numerically to previously established values. However, the cones in our study area are several hundred meters high, which is in disagreement with previously established theoretical considerations (Wood, 1979b; Wilson and Head, 1994).

Several types of monogenetic volcanoes on Earth (spatter cones, rootless cones and scoria/cinder cones) have a similar  $W_{CR}/W_{CO}$  ratio of  $\sim 0.4$  (Wood, 1979a). It is impossible, therefore, to classify an investigated edifice as scoria or cinder cone only from the  $W_{CR}/W_{CO}$  ratio alone. Generally, different types of volcanic cones cannot be separated from each other by using a single morphometric factor such as cone basal diameter or cone height (Wood, 1979a). Moreover, climatic conditions and the grain size distribution might have an influence on morphometry (Wood, 1980b; Riedel et al., 2003; Rodriguez et al., 2010) and morphometric ratios are an indication of the average shape and construct structure, but do not relate to a typical cone-forming process (Kervyn et al., 2012). Independent information on the geological context is required to further distinguish between different cone types. Our observations show that flow-like features are associated with several cones (Fig. 2.3a and 2.3c). We interpret these lobate deposits as lava flows, similar to terrestrial lava flows associated with scoria cones (Fig. 2.3d and 2.3e). The association of cones with lava flows, typical for terrestrial scoria cones (Pioli et al., 2009) or spatter cones, strongly supports an origin of the cones as pyroclastic cones. This interpretation excludes an origin of the cones as rootless cones, because these are rootless edifices without any connection to deeper magma sources. Moreover, the dimensions of rootless cones are several times smaller than those of the investigated cones. Spatter cones are another alternative, but Wood (1979a) points out that, in general, all morphometric parameters have lower values for spatter cones as compared to scoria or cinder cones. For example, the *mean* cone basal diameter of spatter cones on Earth is one order of magnitude smaller than that of scoria or cinder cones, and

the volume range is typically smaller by two orders of magnitude. These differences might suggest that spatter emplacement was not the dominant mode of formation for these cones as opposed to scoria emplacement.

The larger basal diameters and heights of the cones in our study area as compared to pyroclastic cones on Earth could be accounted for by larger erupted magma volumes than for terrestrial pyroclastic cones. The basically identical  $W_{CR}/W_{CO}$  ratio is not in agreement with theoretical predictions by Wilson and Head (1994), however, it is consistent with the results of Wood (1979b). Based on the morphological and morphometrical arguments presented above and the association of cones with lava flows, we interpret the cones as pyroclastic (scoria) cones. The cones and the associated lava flows are superposed on a material with rough texture, which is again superposed on the fractured basement. We interpret the rough material as a mixture of distal pyroclastic deposits and lava flows. Our interpretation of the geologic context of the volcanic field is shown in Fig. 2.8. Although it is not possible to determine the duration of the formation of single cones, the similarity to monogenetic volcanic fields on Earth tentatively suggests that the martian cones might be monogenetic volcanoes as well.

The spatial arrangement of the cones is obviously controlled by the grabens of Ulysses Fossae (Fig. 2.1, 2.2, 2.7, 2.8), an extensional fracture zone that is characterized by several sets of normal faults that commonly form grabens (Scott and Dohm, 1990). The orientation of the faults is generally NW, N, and NNE, but a few faults also trend roughly WSW-ENE. The cones are aligned along fractures trending NNW (Fig. 2.2), and an eruptive fissure (Fig. 2.3c) is also parallel to this fault trend. Cone alignment on Earth is commonly controlled by regional and local tectonic patterns such as defined by fault and rift zones (e.g., Connor and Conway, 2000; Bonali et al., 2011). It seems possible that the cone-related volcanic activity was directly related to the extensional stress in the martian lithosphere. Analogies are

well known from the Earth, where rifting will typically start as a broad zone of extension, but will eventually transition towards a narrow zone of focused magmatic intrusion (e.g., Rooney et al., 2011). Magma can ascend via dikes to produce surface volcanism, which can be manifested as aligned scoria cones as it is observed, e.g., in the Main Ethiopian Rift (Rooney et al., 2011). In this case, the magmatism would be contemporaneous to the rifting and be an integral part of the rifting itself (magma-assisted rifting; e.g., Kendall et al., 2005). Alternatively, the distribution of vents in monogenetic volcanic fields may be controlled by the reactivation of older structures that enable a more favorable magma ascent (e.g., Cebriá et al., 2011), a mechanism which was also suggested for Mars (Bleacher et al., 2009). Currently it is not possible to decide which of the two options applies to the study area. Detailed age dating would be a way to solve this question, but this appears difficult due to the inherent problems in dating small-scale features with a thick dust cover.

Terrestrial pyroclastic cones are formed by scoria clasts and are susceptible to erosion. Several of the cones in the study area, mainly in its southern part, are relatively well preserved. This observation, together with the well-developed associated lava flows, suggests that there was no significant erosion since their emplacement. Cones in the northern part of the study area appear more degraded, and no associated lava flows can be identified. On Earth, the degradational evolution of pyroclastic cones is correlated with the amount of time they have been exposed to erosion (Hooper and Sheridan, 1998), and the  $H_{CO}/W_{CO}$  ratio as well as the maximum and average slope angles of their flanks decrease with time (e.g., Dohrenwend et al., 1986; but note the limitations of this method to estimate relative cone age by Favalli et al., 2009a). Indeed, the  $H_{CO}/W_{CO}$  ratio of cones in the study area is generally increasing from north to south (Tab. 2.2). By analogy, we conclude that the cones in the north part of the study area are older than those in the southern part. The northern cones appear much more degraded (see also Tab. 2.2), and since erosion rates on Mars are very low

after the Noachian (Golombek et al., 2006), this suggests that the formation of the cones in the entire study area spans an extended period of time. The relatively small number of cones does not seem to be in disagreement with this notion. Firstly, the original number of cones might have been larger, but most of them have been eroded beyond identification. Secondly, the number of cones in a volcanic field does not correspond with its longevity (Connor and Conway, 2000), so even a field with a small number of vents might have been long-lived.

Pyroclastic cones are typically formed by Hawaiian and/or Strombolian eruptions (e.g., Head and Wilson, 1989; Vergnolle and Mangan, 2000). Strombolian explosive eruptions are characterized by the more or less intermittent formation and bursting of a gas bubble close to the surface (e.g., Blackburn et al., 1976; Wilson, 1980). Different models exist to describe the mechanisms of Hawaiian-style lava fountaining (e.g., Wilson, 1980; Wilson and Head, 1981; Jaupart and Vergnolle, 1988; see review by Parfitt, 2004). It is not possible to distinguish between the two eruptive styles on Mars on the basis of cone morphology in our study area. Moreover, there is a continuum between these two styles of volcanism, and it is common that one type of activity changes to the other one during an eruption (Parfitt and Wilson, 1995; Vergnolle and Mangan, 2000). The observation of lava flows and eruptive fissures (Fig. 2.3) suggests that at least some stages in the eruptions might have been dominated by fire fountaining, leading to the formation of a pyroclastic cone, lava flows and rootless flows according to the scheme discussed by Head and Wilson (1989; see their Fig. 7). Nevertheless, some possible aspects of the eruptions responsible for cone formation in the Ulysses Fossae regions can be discussed.

The observed style of eruptive activity in the study area differs markedly from that of younger plain-style volcanism in Tharsis and Elysium, which is predominantly effusive (Hauber et al., 2009a; Vaucher et al., 2009b). In general, the explosivity of a basaltic eruption

is controlled by various parameters, such as the volatile content of the magma, magma viscosity and magma rise speed, and interaction of magma with ground water or ground ice (e.g., Wilson, 1980; Roggensack et al., 1997; Pioli et al., 2009). Materials forming pyroclastic cones can originate by explosive fragmentation from ascending magma by two main processes. Firstly, material is forming from rapid exsolution and decompression of magmatic volatiles, and secondly by interaction of groundwater with magma, or by a combination of these two styles (Vespermann and Schmincke, 2000). The first mechanism was theoretically discussed by Wilson and Head (1994), and the lower atmospheric pressure on Mars would promote the explosivity of martian eruptions under current atmospheric conditions. The same authors, however, predict that the higher ejection velocities of the fragmented particles would lead to a wider dispersal of eruption products, thus making the identification of deposits difficult (Francis and Wood 1982; Wilson and Head, 2007). The observed morphology of the cones in our study area, with readily identified pyroclastic material, does not agree with these predictions. Partly this might be due to a thicker atmosphere at the time of cone formation (perhaps higher CO<sub>2</sub> contents from polar cap sublimation caused by astronomical forcing of climate changes; Phillips et al., 2011), but it is not clear if plausible increases in atmospheric pressure would be a sufficient explanation.

The difference between the eruptive style in the study area and in the younger volcanic plains is obvious, but there is no straightforward explanation. Volcanic fields with morphologies similar to the study area might have been more widespread in the past, but might now be buried under younger lava plains. Magma viscosity might have been different, but due to the thick dust cover there are no compositional data from orbiting spectrometers. The morphology of the lava flows might be an indirect indicator of more viscous magma (which would promote explosive activity), since the flows are relatively short and appear to have steep flow fronts. This lava morphology is distinct from that typically observed

in most young plain-style regions of Tharsis and Elysium, where lavas seem to have low viscosities (e.g., Vaucher et al., 2009b; Hauber et al., 2011). Large and long-lived magma chambers beneath the study area might have allowed magma to differentiate to more silicic compositions, and stratification together with volatile differentiation would potentially have favor explosive activity at least in the initial stages of an eruption (Mitchell and Wilson, 2001). Without additional evidence, however, this explanation is very speculative.

## **2.8. Conclusions**

1) Based on morphological and morphometrical analyses, we interpret an assemblage of landforms in Tharsis as a volcanic field with pyroclastic cones and associated lava flows. This result is consistent with the hypothesis that explosive basaltic volcanism should be common on Mars. It is surprising that this is the only well-preserved field of this kind seen so far on Mars, given the fact that pyroclastic cones are the most common volcanoes on Earth (Wood, 1980a; Valentine and Gregg, 2008). A possible explanation is that similar volcanic fields existed in the past, but were subsequently buried by younger volcanic deposits. If true, this might imply a gradual change in eruption style in Tharsis, from more explosive towards more effusive volcanism.

2) The spatial distribution of cones is controlled by regional tectonic trends, and cones are aligned along NNW-trending normal faults and grabens. It is not clear whether the volcanic activity was contemporaneous with the faulting, or whether the magmatism postdated the tectonism, with dikes ascending along pre-existing lines of structural weakness. Faulted volcanic substrate beneath the cones suggests that at least some of the faulting was post-volcanic.

3) The observed evidence for physiological diversity of martian volcanism is still growing (see also Lanz et al., 2010). The morphologic detection of volcanic centres in dust-free areas might enable the detection of further hydrothermal deposits (Skok et al., 2010).

## **Acknowledgements**

Discussions with Thomas Platz helped to improve the manuscript. We appreciate two detailed and constructive reviews by Jacob Bleacher and Julia Lanz. We thank to Felix Jagert for his help with ArcGIS and Thomas Kneissl for help with CraterTool. This study was partly supported by the Helmholtz Alliance ‘Planetary Evolution and Life’ and by grant ME09011 of the program KONTAKT of the Ministry of Education of the Czech Republic.

## References

- Anderson, R. C., Dohm, J. M., Golombek, M. P., Haldemann, A. F. C., Franklin, B. J., Tanaka, K. L., Lias, J., Peer, B., 2001. Primary centers and secondary concentrations of tectonic activity through time in the western hemisphere of Mars, *J. Geophys. Res.* 106, 20,563–20,585, doi:10.1029/2000JE001278.
- Blackburn, E. A., Wilson, L., Sparks, R. S. J., 1976. Mechanisms and dynamics of Strombolian activity. *J. Geol. Soc. (Lond.)* 132, 429–440.
- Bleacher, J.E., Greeley, R., Williams, D.A., Cave, S.R., Neukum, G., 2007. Trends in effusive style at the Tharsis Montes, Mars, and implications for the development of the Tharsis province. *J. Geophys. Res.*, 112, E09005, doi:10.1029/2006JE002873.
- Bleacher, J. E., Glaze, L. S., Greeley, R., Hauber, E., Baloga, S. M., Sakimoto, S. E. H., Williams, D. A., Glotch, T. D., 2009. Spatial and alignment analyses for a field of small volcanic vents south of Pavonis Mons and implications for the Tharsis province, Mars. *J. Volcanol. Geotherm. Res.* 185, 96–102.
- Bonali, F. L., Corazzato, C., Tibaldi, A. (2011) Identifying rift zones on Volcanoes: an example from La Réunion Island, Indian Ocean. *Bull. Volcanol.* 73, 347–366.
- Carr M. H., Greeley, R., Blasius, K. R., Guest, J. E., Murray, J. B., 1977. Some Martian volcanic features as viewed from the Viking Orbiters. *J. Geophys. Res.* 82, 3985–4015.
- Carn, S. A., 2000. The Lamongan volcanic field, East Java, Indonesia: physical volcanology, historic activity and hazards. *J. Volcanol. Geotherm. Res.* 95, 81–108.
- Cebriá, J. M., Martín-Escorza, C., López-Ruiz, J., Morán-Zenteno, D. J., Martiny, B. M., 2011. Numerical recognition of alignments in monogenetic volcanic areas: Examples from the Michoacán-Guanajuato Volcanic Field in Mexico and Calatrava in Spain. *J. Volcanol. Geotherm. Res.* 201, 73–82.
- Chapman, M. G., 2002. Layered, massive and thin sediments on Mars: possible Late Noachian to Late Amazonian tephra? In: Smellie, J. L., Chapman, M. G. (Eds.), *Volcano-Ice Interaction on Earth and Mars*, Geological Society, London, Special Publication 202, pp. 273-293, doi: 10.1144/GSL.SP.2002.202.01.14.
- Crater Analysis Techniques Working Group, 1979. Standard techniques for presentation and analysis of crater size-frequency data. *Icarus* 37, 467–474.
- Connor, C. B., Conway, F. M., 2000. Basaltic Volcanic Fields. In: Sigurdsson, H. (Ed.), *Encyclopedia of Volcanoes*, Academic Press, San Diego, pp. 331–343.
- Corazzato, C., Tibaldi, A., 2006. Fracture control on type, morphology and distribution of parasitic volcanic cones: An example from Mt. Etna, Italy. *J. Volcanol. Geotherm. Res.* 158, 177–194.
- Crown, D. A., Greeley, R., 1993. Volcanic geology of Hadriaca Patera and the eastern Hellas region of Mars. *J. Geophys. Res.* 98, 3431–3451.
- Dehn J., Sheridan, M. F., 1990. Cinder Cones on the Earth, Moon, Mars, and Venus: A computer model. *Lunar Planet. Sci.* XXI, 270 (abstract).
- Dohrenwend, J. C., Wells, S. G., Turrin, B. D., 1986. Degradation of Quaternary cinder cones in the Cima volcanic field, Mojave Desert, California. *Geol. Soc. Am. Bull.* 97, 421–427.
- Edgett, K. S., 1990. Possible cinder cones near the summit of Pavonis Mons, Mars. *Lunar Planet. Sci.* XXI, 311–312.
- Fagents, S. A., Wilson, L., 1996. Numerical modeling of ejecta dispersal from transient volcanic explosions on Mars. *Icarus* 123, 284–295.
- Fagents, S. A., Thordarson, T., 2007. Rootless volcanic cones in Iceland and on Mars. In: Chapman, M. (Ed.), *The Geology of Mars*, Cambridge University Press, Cambridge, pp. 151-177.
- Favalli, M., Mazzarini, F., Pareschi, M.T., Boschi, E., 2009. Topographic control on lava flow paths at Mt. Etna (Italy): Implications for hazard assessment. *J. Geophys. Res.* 114, F01019, doi: 10.1029/2007JF000918

- Francis, P. W., Wood, C. A., 1982. Absence of silicic volcanism on Mars - Implications for crustal composition and volatile abundance. *J. Geophys. Res.* 87, 9881–9889.
- Frey, H., Jarosewich, M., 1982. Subkilometer Martian volcanoes - Properties and possible terrestrial analogs. *J. Geophys. Res.* 87, 9867–9879.
- Golombek, M. P., et al., 2006. Erosion rates at the Mars Exploration Rover landing sites and long-term climate change on Mars. *J. Geophys. Res.* 111, E12S10, doi: 10.1029/2006JE002754.
- Greeley, R., 1973. Mariner 9 photographs of small volcanic structures on Mars. *Geology* 1, 175–180.
- Greeley, R., Crown, D. A., 1990. Volcanic geology of Tyrrhena Patera, Mars. *J. Geophys. Res.* 95, 7133–7149.
- Greeley, R., Spudis, P. D., 1981. Volcanism on Mars. *Rev. Geophys. Space Phys.* 19, 13–41.
- Gregg, T. K. P., Williams, S. N., 1996. Explosive mafic volcanoes on Mars and Earth: Deep magma sources and rapid rise rate. *Icarus* 122, 397–405.
- Gregg, T. K. P., Farley, M. A., 2006. Mafic pyroclastic flows at Tyrrhena Patera, Mars: Constraints from observations and models. *J. Volcanol. Geotherm. Res.* 155, 81–89.
- Grosse, P., van Wyk de Vries, B., Euillades, P. A., Kervyn, M., Petrinovic, I. A., 2011. Systematic morphometric characterization of volcanic edifices using digital elevation models. *Geomorphology*, in press, doi: 10.1016/j.geomorph.2011.06.001.
- Hartmann W. K. and Neukum G. (2001) Cratering Chronology and the Evolution of Mars, *Space Science Reviews*, v. 96, Issue 1/4, p. 165-194.
- Hasenaka, T., Carmichael, I. S. E., 1985a. A compilation of location, size, and geomorphological parameters of volcanoes of the Michoacán-Guanajuato volcanic field, Central Mexico. *Geof. Int.* 24-4, 577–607.
- Hasenaka, T., Carmichael, I. S. E., 1985b. The cinder cones of Michoacán–Guanajuato, central Mexico: their age, volume and distribution, and magma discharge rate. *J. Volcanol. Geotherm. Res.* 25, 104–124.
- Hauber E., Bleacher J., Gwinner, K., Williams D., Greeley R., 2009. The topography and morphology of low shields and associated landforms of plains volcanism in the Tharsis region of Mars, *J. Volcanol. Geotherm. Res.* 185, 69–95.
- Hauber, E., Brož, P., Jagert, F., Jodłowski, P., Platz, T., 2011. Very recent and wide-spread basaltic volcanism on Mars, *Geophys. Res. Lett.* 28, L10201, doi:10.1029/2011GL047310.
- Head, J. W., Wilson, L., 1989. Basaltic pyroclastic eruptions: influence of gas release patterns and volume fluxes on fountain structure, and the formation of cinder cones, spatter cones, rootless flows, lava ponds and lava flows. *J. Volcanol. Geotherm. Res.* 37, 261–271.
- Hodges, C. A., Moore, H. J., 1994. Atlas of volcanic features on Mars. U.S. Geol. Survey Professional Paper 1534, U.S. Govt. Printing Office, Washington DC, 194 pages.
- Hooper, D. M., Sheridan, M. F., 1998. Computer-simulation models of scoria cone degradation. *J. Volcanol. Geotherm. Res.* 83, 241–267.
- Hynek, B. M., Phillips, R. J., Arvidson, R. E., 2003. Explosive volcanism in the Tharsis region: Global evidence in the Martian geologic record. *J. Geophys. Res.* 108, CiteID 5111, doi: 10.1029/2003JE002062.
- Inbar, M., Risso, C., 2001. A morphological and morphometric analysis of a high density cinder cone volcanic field — Payun Matru, south-central Andes, Argentina. *Zeitschrift für Geomorphologie* 45, 321–343.
- Inbar, M., Gilichinsky, M., Melekestsev, I., Melnikov, D., Zaretskaya, N., 2011. Morphometric and morphological development of Holocene cinder cones: A field and remote sensing study in the Tolbachik volcanic field, Kamchatka. *J. Volcanol. Geotherm. Res.* 201, 301–311.
- Ivanov, B.A.. 2001. Mars/Moon Cratering Rate Ratio Estimates, *Space Science Reviews*, v. 96, Issue 1/4, p. 87-104.

- Jaumann, R., et al., 2007. The high-resolution stereo camera (HRSC) experiment on Mars Express: instrument aspects and experiment conduct from interplanetary cruise through the nominal mission. *Planet. Space Sci.* 55, 928–952.
- Jaupart, C., Vergnolle, S., 1988. Laboratory models of Hawaiian and Strombolian eruptions. *Nature* 331, 58–60.
- Kendall, J.-M., Stuart, G. W., Ebinger, C. J., Bastow, I. D., Keir, D., 2005. Magma-assisted rifting in Ethiopia. *Nature* 433, 146–148.
- Kerber, L., Head, J. W., Madeleine, J. B., Wilson, L., Forget, F., 2010. The distribution of ash from ancient explosive volcanoes on Mars. *Lunar Planet. Sci. XLI, LPI Contribution No. 1533*, abstract 1006.
- Kervyn, M., Ernst, G. G. J., Carracedo, J.-C., Jacobs, P. (2011). Geomorphometric variability of “monogenetic” volcanic cones: Evidence from Mauna Kea, Lanzarote and experimental cones. *Geomorphology*, in press, doi: 10.1016/j.geomorph.2011.04.009.
- Keszthelyi, L., Jaeger, W., McEwen, A., Tornabene, L., Beyer, R.A., Dundas, C., Milazzo, M., 2008. High Resolution Imaging Science Experiment (HiRISE) images of volcanic terrains from the first 6 months of the Mars Reconnaissance Orbiter primary science phase. *J. Geophys. Res.* 113, E04005. doi:10.1029/2007JE002968.
- Keszthelyi, L. P., Jaeger, W. L., Dundas, C. M., Martínez-Alonso, S., McEwen, A. S., Milazzo, M. P., 2010. Hydrovolcanic features on Mars: Preliminary observations from the first Mars year of HiRISE imaging. *Icarus* 205, 211–229.
- Kneissl, T. van Gasselt S., Neukum G. 2010. Map-projection-independent crater size-frequency determination in GIS environments—New software tool for ArcGIS. *Planet Space Sci.* ,doi:10.1016/j.pss.2010.03.015, in press.
- Lanagan, P.D., McEwen, A.S., Keszthelyi, L.P., Thordarson, T., 2001. Rootless cones on Mars indicating the presence of shallow equatorial ground ice in recent times. *Geophys. Res. Lett.* 28, 2365–2368.
- Lanz, J. K., Wagner, R., Wolf, U., Kröcher, J., Neukum, G., 2010. Rift zone volcanism and associated cinder cone field in Utopia Planitia, Mars. *J. Geophys. Res.* 115, E12019, doi: 10.1029/2010JE003578.
- McEwen, A. S., et al., 2007. Mars Reconnaissance Orbiter's High Resolution Imaging Science Experiment (HiRISE). *J. Geophys. Res.* 112, E05S02, doi: 10.1029/2005JE002605.
- Malin, M. C., et al., 2007. Context camera investigation on board the Mars Reconnaissance Orbiter. *J. Geophys. Res.* 112, E05S04, doi:10.1029/2006JE002808.
- Mandt, K. E., de Silva, S. L., Zimbelman, J. R., Crown, D. A., 2008. Origin of the Medusae Fossae Formation, Mars: Insights from a synoptic approach. *J. Geophys. Res.* 113, E12011, doi: 10.1029/2008JE003076.
- McKnight, S. B., Williams S. N., 1997. Old cinder cone or young composite volcano? The nature of Cerro Negro, Nicaragua. *Geology* 25, 339–342.
- Michael, G.G., Neukum, G., 2010. Planetary surface dating from crater size–frequency distribution measurements: Partial resurfacing events and statistical age uncertainty. *Earth Planet. Sci. Lett.* 294, 223–229.
- Mitchell, K.L., Wilson, L., 2001. Explosive volcanic eruptions on Mars: Misconceptions and new insights. *Lunar Planet. Sci. XXXII*, abstract 1190.
- Mouginis-Mark, P. J., Wilson, L., Zuber, M. T., 1992. The Physical Volcanology of Mars. In: Kieffer, H.H., Jakosky, B.M., Snyder, C.W., Matthews, M.S. (Eds.), *Mars*, Univ. of Arizona Press, Tucson, pp. 424–452.
- Nakamura, K., 1977. Volcanoes as possible indicators of tectonic stress orientation – principle and proposal. *J. Volcanol. Geotherm. Res.* 2, 1–16.
- Parfitt, E. A., 2004. A discussion of the mechanisms of explosive basaltic eruptions. *J. Volcanol. Geotherm. Res.* 134, 77–107.

- Parfitt E. A., Wilson, L., 1995. Explosive volcanic eruptions-IX. The transition between Hawaiian-style lava fountaining and Strombolian explosive activity. *Geophys. J. Int.* 121, 226–232.
- Parfitt E. A., Wilson, L., 2008. *Fundamentals of Physical Volcanology*. Blackwell, Oxford, 256 pages.
- Phillips, R.J., et al., 2011. Massive CO<sub>2</sub> ice deposits sequestered in the south polar layered deposits of Mars. *Science*, 332, 838–841.
- Pike, R. J., 1978. Volcanoes on the inner planets: Some preliminary comparisons of gross topography. *Proc. Lunar Planet. Sci. Conf. IX*, 3239–3273.
- Pioli, L., Azzopardi, B. J., Cashman, K. V., 2009. Controls on the explosivity of scoria cone eruptions: Magma segregation at conduit junctions. *J. Volcanol. Geotherm. Res.* 186, 407-415.
- Plescia, J. B., 1994. Geology of the small Tharsis volcanoes: Jovis Tholus, Ulysses Patera, Biblis Patera, Mars. *Icarus* 111, 246–269
- Plescia, J. B., 2004. Morphometric properties of Martian volcanoes. *J. Geophys. Res.* 109, E03003, doi: 10.1029/2002JE002031.
- Porter S. C., 1972. Distribution, morphology, and size frequency of cinder cones on Mauna Kea Volcano, Hawaii. *Bull. Geol. Soc. Amer.* 83, 3607–3612.
- Riedel, C., Ernst, G. G. J., Riley, M., 2003. Controls on the growth and geometry of pyroclastic constructs. *J. Volcanol. Geotherm. Res.* 127, 121–152.
- Rodriguez, S.R., Morales-Barrera, W., Layer, P., González-Mercado, E., 2010. A quaternary monogenetic volcanic field in the Xalapa region, eastern Trans-Mexican volcanic belt: Geology, distribution and morphology of the volcanic vents. *J. Volcanol. Geotherm. Res.* 197, 149–166.
- Roggensack, K., Hervig, R. L., McKnight, S. B., Williams, S. N., 1997. Explosive basaltic volcanism from Cerro Negro volcano: Influence of volatiles on eruptive style. *Science* 277, 1639–1642.
- Rooney, T., Bastow, I.D., Keir, D., 2011. Insights into extensional processes during magma assisted rifting: Evidence from aligned scoria cones and maars. *J. Volcanol. Geotherm. Res.* 201, 83-96, doi: 10.1016/j.jvolgeores.2010.07.019
- Scott, D. H., Dohm, J. M., 1990. Faults and ridges - Historical development in Tempe Terra and Ulysses Patera regions of Mars. *Proc. Lunar Planet. Sci.* XX, 503-513.
- Scott, D. H., Tanaka, K. L., 1986. Geologic map of the western equatorial region of Mars. U.S. Geological Survey Miscellaneous Investigation Series Map I-1802-A, scale 1:15,000,000.
- Settle, M., 1979. The structure and emplacement of cinder cone fields. *Am. J. Sci.* 279, 1089–1107.
- Skok, J.R., Mustard, J.F., Ehlmann, B.L., Milliken, R.E., Murchie, S.L., 2010. Silica deposits in the Nili Patera caldera on the Syrtis Major volcanic complex on Mars. *Nature Geosci.* 3, 838-841.
- Smith, D. E., et al., 2001. Mars Orbiter Laser Altimeter: experiment summary after the first year of global mapping of Mars. *J. Geophys. Res.* 106, 23,689–23,722.
- Squyres, S. W. et al., 2008. Pyroclastic activity at Home Plate in Gusev Crater, Mars. *Science* 316, 738–742.
- Tibaldi, A., 1995. Morphology of pyroclastic cones and tectonics. *J. Geophys. Res.* 100, 24,521–24,535.
- Valentine, G. A., Gregg, T. K. P., 2008. Continental basaltic volcanoes - processes and problems. *J. Volcanol. Geotherm. Res.* 177, 857–873, doi: 10.1016/j.jvolgeores.2008.01.050.
- Vaucher, J., Baratoux, D., Toplis, M. J., Pinet, P., Mangold, N., Kurita, K., 2009. The morphologies of volcanic landforms at Central Elysium Planitia: Evidence for recent and fluid lavas on Mars. *Icarus*, 200, 39–51.
- Vergnolle, S., Mangan, M., 2000. Hawaiian and Strombolian eruptions. In: Sigurdsson, H. (Ed.), *Encyclopedia of Volcanoes*, Academic Press, San Diego, pp. 447–461.

- Vespermann, D., Schmincke, H.-U., 2000. Scoria cones and tuff rings. In: Sigurdsson, H. (Ed.), *Encyclopedia of Volcanoes*, Academic Press, San Diego, pp. 683–694.
- Williams, D. A., Greeley, R., Zuschneid, W., Werner, S. C., Neukum, G., Crown, D. A., Gregg, T. K. P., Gwinner, K., Raitala, J., 2007. Hadriaca Patera: Insights into its volcanic history from Mars Express High Resolution Stereo Camera. *J. Geophys. Res.* 112, E10004, doi: 10.1029/2007JE002924.
- Williams, D. A., Greeley, R., Werner, S. C., Michael, G., Crown, D. A., Neukum, G., Raitala, J., 2008. Tyrrhena Patera: Geologic history derived from Mars Express High Resolution Stereo Camera. *J. Geophys. Res.* 113, E11005, doi: 10.1029/2008JE003104.
- Wilson, L., 1980. Relationships between pressure, volatile content and ejecta velocity in three types of volcanic explosion. *J. Volcanol. Geotherm. Res.* 8, 297–313.
- Wilson, L., Head, J. W., 1981. Ascent and eruption of basaltic magma on the Earth and Moon. *J. Geophys. Res.* 86, 2971–3001.
- Wilson, L., Head, J.W., 1994. Review and analysis of volcanic eruption theory and relationships to observed landforms: *Rev. Geophys.* 32, 221–263, doi: 10.1029/94RG01113.
- Wilson, L., Head, J. W., 2007. Explosive volcanic eruptions on Mars: Tephra and accretionary lapilli formation, dispersal and recognition in the geological record. *J. Volcan. Geotherm. Res.* 163, 83–97.
- Wood C. A., 1979a. Monogenetic volcanoes of the terrestrial planets. *Proc. Lunar Planet. Sci.* XX, 2815–2840.
- Wood, C. A., 1979b. Cinder cones on Earth, Moon and Mars. *Lunar Planet. Sci.* X, 1370–1372 (abstract).
- Wood C. A., 1980a. Morphometric evolution of cinder cones. *J. Volcanol. Geotherm. Res.* 7, 387–413.
- Wood C. A., 1980b. Morphometric analysis of cinder cone degradation. *J. Volcanol. Geotherm. Res.* 8, 137–160.
- Zimbelman, J. R., 2000. Volcanism on Mars. In: Sigurdsson, H. (Ed.), *Encyclopedia of Volcanoes*, Academic Press, San Diego, pp. 771–783.
- Zuber, M. T., Smith, D. E., Solomon, S. C., Muhleman, D. O., Head, J. W., Garvin, J. B., Abshire, J. B., Bufton, J. L., 1992. The Mars Observer Laser Altimeter investigation. *J. Geophys. Res.* 97, 7781–7797.